# Accepted Manuscript


Kinetic modeling of the γ phase in Ti-Al-Nb alloys

Ida S. Berglund, Zachary L. Bryan, Michele V. Manuel

PII: S0925-8388(17)32769-X

DOI: 10.1016/j.jallcom.2017.08.041

Reference: JALCOM 42798

To appear in: *Journal of Alloys and Compounds*

Received Date: 22 October 2016

Revised Date: 10 July 2017

Accepted Date: 6 August 2017

Please cite this article as: I.S. Berglund, Z.L. Bryan, M.V. Manuel, Kinetic modeling of the γ phase in Ti-Al-Nb alloys, *Journal of Alloys and Compounds* (2017), doi: 10.1016/j.jallcom.2017.08.041.

# Kinetic modeling of the γ phase in Ti-Al-Nb alloys

Ida S. Berglund[1], Zachary L. Bryan[1], Michele V. Manuel[1]
[1]*Department of Materials Science and Engineering, University of Florida, Gainesville, FL 32611,* USA

**Abstract**
A mobility database for the γ-TiAl phase in the Ti-Al-Nb system was created by a critical assessment of experimental diffusion data found in literature. Optimization of mobilities and diffusion modeling was performed using the DICTRA (DIffusion Controlled TRAnsformations) software. Agreement was found between the experimental and calculated diffusion coefficients. The database was further validated with a diffusion couple consisting of 46Ti-54Al and 31Ti-55Al-14Nb alloys. The experimental data and final optimization revealed Nb-dependent effects on the diffusivities of all three elements. The Nb diffusivity increases with Nb content, and the Ti and Al diffusivities vary with composition in both binary and ternary alloys.

**Keywords:** Titanium aluminide, niobium, DICTRA, diffusion, database

## Introduction

The development of new materials is today based on quantitative conceptual design where processing and structures are modeled to predict the properties and performance of materials using the Integrated Computational Materials Engineering (ICME) approach. In order to predict microstructural evolution at the micro- to mesoscale, thermodynamic and kinetic database development are of utmost importance for these models and predictions.

Titanium aluminides are relevant for a wide range of applications, for example in the chemical, automotive, medical and power industries[1]. One particular application is found in gas turbine engines as potential substitute for the currently used Ni-based superalloys[2, 3]. Titanium aluminides have lower density, which would significantly increase fuel efficiency, decreasing cost and environmental effects. While Ti-based alloys are already partly used in these engines, they are limited to the low-temperature regions due to inadequate high-temperature properties[2]. Microstructure stability and creep resistance are crucial in these applications, both of which are diffusion-controlled processes at elevated temperature[4]. Previous alloy development has primarily focused on the γ-TiAl phase, as well as its combination with $\alpha_2$-$Ti_3Al$ to form a lamellar structure. Although the lamellar-type alloys have excellent creep behavior up to 800°C, the ordered structure of these alloys make them brittle[1]. Alloying with beta-stabilizing elements, such as Nb, Cr or Mo, can improve their ductility; however, due to poor long term stability of $\alpha_2$, much focus has been directed toward γ-based alloys[1]. Recent studies have acknowledged the potential use of Nb addition to achieve improved high temperature properties in γ-TiAl[5, 6]. Experimental work has showed that the addition of Nb can potentially increase the high temperature strength, ductility and strain rate sensitivity of these alloys[7]. It has also been shown that high temperature mechanical properties can be achieved with Nb addition, without compromising the oxidation resistance by reducing the Al content[6]. Further, it has been suggested that a desirable microstructure can be achieved by controlling the precipitation of γ-TiAl and σ-$Nb_2Al$ phases from the β-phase[8]. While the thermodynamics of these systems are relatively well understood, the kinetics are less known, especially in ternary or higher order systems. A kinetic database could significantly accelerate the development process of these alloys.

Due to long history of the use of titanium aluminides in various applications, the literature is comprehensive, including both experimental diffusion data and theoretical kinetic predictions.

For example, Mishin and Herzig[9] reviewed the experimental and theoretical experiments on diffusivities in the phases of the Ti-Al system, including discussions on atomic site preferences and diffusion mechanisms, as well as defect formation energies in γ-TiAl. Despite being exhaustively studied, there is currently no kinetic database available for this ternary system, aside from the Ti-rich body centered cubic (BCC)[10] and Al-rich face centered cubic (FCC)[11] solid solution phases. Further, there is no kinetic database or assessments for the binary Ti-Al (or ternary TiAlNb) γ-phase face centered tetragonal system. The objective of this work was to critically assess and develop a mobility database for the simulation of diffusion in the binary Ti-Al and ternary Ti-Al-Nb γ-phase.

**Kinetic modeling**

To obtain a complete description of the kinetics in a multicomponent system without making it excessively complex, mobilities can be used, as opposed to diffusivities. This significantly reduces the parameters required to describe the entire diffusivity matrix, assuming it can be coupled with a thermodynamic database. According to Andersson end Ågren[12], the diffusivity can be described by a kinetic factor and a thermodynamic factor. Assuming a lattice-fixed frame of reference and a vacancy exchange mechanism, the composition-dependent diffusion coefficient is a product of the two, as shown in equation 1:

$$D_{kj}^{L} = \sum_i M_{ki} \frac{\partial \mu_i}{\partial x_j} \quad (1)$$

where M is the mobility, i is the matrix specie, k and j refers to the gradient and diffusion specie, respectively, μ is the chemical potential, and x is the mole fraction[12]. The partial derivative of the chemical potential with respect to composition, the thermodynamic factor, is readily available from a multicomponent thermodynamic database. By assuming that the off-diagonal terms in the diffusivity matrix are zero[12], and there are no magnetic effects, the mobility of element i, $M_i$, can be described by equation 2:

$$M_i = M_i^0 \frac{1}{RT} exp\left(-\frac{Q_i}{RT}\right) \quad (2)$$

where R is the gas constant, T is the temperature, and Q is the activation energy for diffusion in the given phase. $M_i^0$ is a function of the jump frequency and distance, dependent on composition, temperature and pressure. In the DICTRA notation, the mobility parameters can be grouped into one parameter $\Psi_i = -Q_i$ and $RTlnM_i^0$ . The composition dependence of the mobility for a non-ordered phase is described by Redlich-Kister polynomials and power series expansion following the CALPHAD approach[12, 13];

$$\Psi_i = \sum_j x_j Q_i^j + \sum_p \sum_{j>p} x_p x_j \sum_k A_i^{pj} \left(x_p - x_j\right)^k + \sum_p \sum_{j>p} \sum_{r>j} x_p x_j x_r (A_i^{pjr} r_{pjr}^s) \quad (3)$$

where $Q_i$ is the activation energy for element i in a given phase, and $A_i^{pj}$ and $A_i^{pjr}$ represents the binary and ternary interaction parameters, respectively, with r, p and j denoting different elements

In this work, the Ti-Al-Nb thermodynamic database assessed by Cupid et al.[14] was used. The γ-phase, an ordered $L1_0$ structure, is described by a two-sublattice configuration, with all three elements present on both sublattices. This lattice configuration necessitated the use of the general model in DICTRA for the current optimization. The limitations with the general model when applied to a stoichiometric phase is that the mobility does not specify the effect of long range ordering in terms of activation energy contribution. If the vacancy concentration is in local equilibrium, and the magnitude of the atomic jump correlation effects are negligible, the assumptions associated with the general model are valid[15, 16].

**Diffusion in the γ-TiAl(Nb) phase**

The diffusion mechanisms taking place in the currently investigated system are not entirely

understood. The γ–phase consists of alternating Ti or Al layers (002 plane) in the $L1_0$ crystal structure[1]. Thus it can be speculated that different mechanisms occur along and perpendicular to the normal axis. Literature[9] also suggests that there is anisotropic diffusion; vacancy mediated jumps within the Ti sublattice is suggested to be the primary mechanism for all three elements, governing their overall diffusivities. Hence, diffusivities are strongly dependent on Ti vacancy concentrations. Further, Herzig et al.[17] suggested that the diffusion of both Al and Ti are dependent on the Ti vacancy concentration only.

Mishin and Herzig[9] calculated formation energies of point defects involving Ti and Al in TiAl using embedded atom analytical expressions for various mechanisms. They concluded that vacancy concentrations of Al and Ti are much more favorable than other defects and that the Ti vacancy is higher than the Al vacancy concentration, regardless of Al content. Diffusion of these elements is thus more likely to occur via substitution on Ti sites. This is also in agreement with first principle calculations; Song et al.[18], for example, concluded that Nb substitutes exclusively on the Ti sublattice. The fact that Al and Nb, with atomic radii of 1.43Å and 2.15Å substitute on the site of the larger atom, in this case Ti (1.47Å), could also be due to their electronic structure governing the diffusivity rather than atomic radius; this was proposed in an early study by Guard and Westbrook[19]. Nose et al.[20], on the other hand, suggested that there are complex correlation effects taking place. Although their single crystal studies determined that diffusion activation energy for Al along [001] is slower than perpendicular to it on the basis of defect activation energies (which supports Al diffusing on the Ti sublattice), they also concluded that activation energies for Ti along [001] are larger than perpendicular to it. Cyclic, anti-site and anti-structural atomic jumps are other mechanisms being discussed in literature[9].

In this work, ascertaining a robust fit to the experimental data was the primary objective, with less focus attributed to the identification of active diffusion mechanisms.

*Experimental data*

Experimental diffusion data from literature was evaluated and used in the current optimization. Tracer diffusivities ($D_i^*$) were given priority in the optimization since the evaluation of these data does not require the use of a thermodynamic description of the systemaccording to the Einstein relation, shown in equation 4[12].

$$D_i^* = RTM_i \tag{4}$$

Intrinsic diffusivity and chemical interdiffusivities, obtained from diffusion couples or multiples, are dependent on thermodynamic parameters, and are measured in the volume fixed frame of reference, as shown in equation 5. Assuming constant partial molar volume, the volume fixed diffusivity, $D^v$, is expressed in terms of mobility according to equation 6, where $\delta_{ik}$ is the Kronecker delta.

$$\widetilde{D}_{kj}^n = D_{kj}^V - D_{kn}^V \tag{5}$$

$$D_{kj}^V = \sum_{i-1}(\delta_{ik} - x_k)x_i M_i \frac{\partial \mu_i}{\partial x_j} \tag{6}$$

In general, there is no discrepancy between the large sets of diffusion data found for Ti and Al diffusion in γ-TiAl. Arrhenius-type temperature dependence is typically seen. Some curvature with temperature has been reported[9, 21], as well as effects of composition[22], suggesting more complex mechanisms taking place.

All data reported below was included in the current optimization, unless otherwise specified. All compositions are in at.%. A summary of these datasets is listed in Table 1.

*Ti in γ -TiAl*

The majority of experimental data found in literature in the system under investigation is on the diffusion of Ti in γ-TiAl. Most studies were performed on bulk diffusion in polycrystalline material where the grain boundary contribution was not considered.

Kroll et al.[23] used the radiotracer method using $^{44}$Ti and serial sectioning to determine the diffusivity of Ti in $Ti_{46}Al_{54}$ between 1154 and 1673 K. This study was later refined by Herzig et al.[24] and expanded to include three compositions; $Ti_{46}Al_{54}$, $Ti_{44}Al_{56}$ and $Ti_{47}Al_{53}$, up to their melting temperatures. They found that there was Arrhenius-type temperature dependence up to 1470 K for $Ti_{44}Al_{56}$ and $Ti_{47}Al_{53}$. $Ti_{46}Al_{54}$ did not have enough data points at low temperatures to conclude temperature dependence. To avoid duplicity in the optimization, only the Herzig data was included since it reported smaller experimental error.

Divinski et al.[21] determined the diffusion of Ti in $Ti_{44}Al_{56}$ using the radiotracer technique with $^{44}$Ti and serial sectioning as well as ion beam sputtering, and found results similar to Herzig et al.

Ikeda et al.[25] also determined the Ti diffusivity in $Ti_{46}Al_{54}$ using radiotracer experiments with $^{44}$Ti and ion beam sputtering, but in single crystals. They determined that there was an order of magnitude faster diffusion of Ti perpendicular to [001] than parallel to it. An average of the two, in the temperature range of 1133 to 1307 K, was used in the current assessment to account for the distribution of orientations in the polycrystalline studies, thereby providing a means for comparison.

*Al in γ -TiAl*

Al tracer diffusivity data is rare due to limited availability of Al isotopes. There are however two studies where tracer substitutes (Ga and In) were used. Herzig et al.[17], used $^{69}$Ga since it was previously shown to well simulate Al self-diffusion in similar stoichiometric Ni-Al phases[26]. Al site preference of Ga is further supported by atom location channeling enhanced microanalysis[27] and density functional theory calculations of TiAl[18]. The Ga tracer diffusivity data in $Ti_{46}Al_{54}$ was obtained using Secondary Ion Mass Spectrometry (SIMS), up to approximately 1515 K.

Nosé et al.[20] used $^{115}$In as a basis for discussing Al diffusion, reasoning that it occupies Al sites according to first principle calculations[18]. The Al diffusion activation energies were discussed along with a model of diffusion in $L1_0$ phases proposed by Ikeda et al.[25] From the single crystal data they suggested that perpendicular to [100], Al primarily diffuses on the Ti sublattice, and that the activation energy parallel to [100] is larger. This is in accordance with the data reported by Ikeda et al.[25]

Interdiffusivities in single phase $Ti_{50}Al_{50}/Ti_{46}Al_{54}$ diffusion couples were determined by Sprengel et al.[28], between 1116 and 1583 K using Electron Probe MicroAnalysis (EPMA). The results suggest temperature dependent Arrhenius behavior, and no significant concentration dependence on the diffusion.

Kainuma et al.[22] used multiphase diffusion couples and EPMA to determine interdiffusivity as a function of Al content, and noted an increase in diffusivity and decreasing activation energy with increasing Al content in the γ-TiAl phase.

It should be pointed out that the previously mentioned study by Kroll et al.[23], on diffusivities from $^{44}$Ti radiotracer, also reported on Al diffusivities. However, the Al diffusivities were calculated using the Darken-Manning equation, which come with inherent errors, along with the previously excluded Ti tracer diffusivity data. Further, Mishin and Herzig[9] calculated diffusivities from the Kroll data using thermodynamic data different from the current study, and presented activation energies different from those reported by others. They further compared the data to their own studies and found that the Kroll data had large errors, which was attributed to short-circuit diffusion. As such, the Kroll Al diffusivity data was excluded in the current assessment.

*Nb in γ –TiAl*

There are two studies of the diffusion of Nb in $Ti_{44}Al_{56}$, both obtained using a combination of $^{93}$Nb SIMS and $^{95}$Nb radiotracer[21, 29], and one study in $Ti_{46}Al_{54}$ using $^{95}$Nb[29]. The use of $^{93}$Nb and SIMS is considered more accurate than $^{95}$Nb radiotracer, since $^{95}$Nb is only available in radiochemical equilibrium with $^{95}$Zr, and as such, the

concentration of $^{95}$Nb is dependent not only on the $^{95}$Zr diffusion, but also on the decay of both isotopes. However, the SIMS technique has inherent temperature limitations. All studies concluded an Arrhenius-type temperature dependence, and Herzig et al.[29] further suggested that the Nb diffusion occurs on the Ti-sublattice via Ti vacancies.

*Ti and Nb in γ-TiAlNb*

Divinski et al.[21, 30] used $^{44}$Ti and $^{95}$Nb radiotracers to determine the respective diffusivities in γ-36Ti-54Al-10Nb alloy, and determined that there is a linear Arrhenius-type temperature dependence for both elements, and that Nb diffuses slower than Ti. They further concluded that above 1000 K, the diffusivity of each of the elements is enhanced compared to their respective diffusivities in binary $Ti_{44}Al_{56}$, attributed to elastic lattice distortion.

**Optimization procedure**

Optimization was performed using the DICTRA software[15]. The Ti, Al and Nb diffusivities were all optimized together using all experimental data. Since Ti, Al and Nb all showed Arrhenius-type temperature dependence, the mobility parameters were expressed accordingly. The two-sublattice configuration enabled a total of 27 base parameters to be optimized. Extra care was taken to evaluate the effect of second-sublattice chemistry changes on the overall fits, and ensure parameters were included to reflect the data accordingly, while aiming to reduce the total number of optimizing parameters. The fitted parameters were then fixed, and an interaction parameter for Al was added to account for temperature-dependence which was not accurately captured in the initial optimization.

**Experimental work**

The diffusion couple technique was utilized to obtain concentration profiles as a function of distance after annealing. The nominal alloy compositions, namely 46Ti-54Al and 31Ti-55Al-14Nb, as indicated in the calculated isothermal section of the phase diagram shown in Figure 1, were selected to enable large Nb concentration while avoiding phase transformation. Elemental forms of Al (99.999%), Ti (99.99%) and Nb (minimum 99.8%) were purchased through Alfa Aesar, and alloys were prepared by mixing high purity elements and arc-melting under a Ti-gettered argon (Ar) atmosphere using a non-consumable tungsten electrode. Both alloys were remelted at least three times to ensure homogeneity. Their compositions were confirmed using EPMA (JEOL Superprobe 733). As-arc-melted buttons were cut into desired shapes and serially ground and polished using a planar to obtain parallel surfaces. The diffusion couple was then clamped together using a custom made jig made of Kovar steel. The couple was then wrapped in tantalum foil and encapsulated in a quartz tube, flushed with Ar, evacuated and sealed under vacuum. The couple was then heat treated at 1000°C for 30 days, followed by air-cooling. The couple was cut perpendicular to the bonding interface and metallographically prepared using alumina and silica slurries. The concentration profile across the surface was then measured using EPMA, using pure Ti, Al and Nb as standards.

**Results and Discussion**

The goal of the current work was to provide a database readily available for simulation of diffusion in γ-TiAlNb. Activation energies reported from the current optimization are an overall representation of whichever mechanism(s) taking place. While more physically relevant diffusion activation energies could be attempted to be represented, the uncertainty in the mechanisms taking place, along with lack of specific description for the ordering effects, limit this approach. Instead, a database representing a robust fit for all available data was created. The optimized parameters are listed in Table 2.

*Ti-Al*

Calculated tracer diffusivities of Al and Ti as function of temperature using the optimized data, are shown in Figures 2 and 3, respectively.

Although overall Arrhenius behavior is observed for Ti and Al tracer diffusion, Divinski et al.[21] detected a slight curvature in the Ti diffusion in

binary TiAl. Mishin and Herzig[9] also observed that above 1473K, the temperature dependence of Ti has a different slope. This curvature was not seen in the other sets of data. While interesting observations, which may suggest shifts in diffusion mechanisms as function of temperature, this curvature was not accounted for in the current optimization.

Experimental data suggests that at higher temperatures there is a slight shift towards slower Ti diffusion with increasing Al content. This is also reflected in the current optimization.

Figure 4 shows the TiAl interdiffusion for different temperatures. As expected, the interdiffusivity increases with increasing temperature. The simulation further shows that the interdiffusivity decreases with increasing Al content. This is contrary to the experimental interdiffusivity data reported by Kainuma et al.[22] (also indicated in Figure 4) who noticed an increase, and the data reported by Sprengel et al.[28] who did not see a concentration dependence on the interdiffusivity.The effect of Al concentration on diffusvity requires further clarification. It should be noted that the interdiffusion data was given lowest priority in the optimization due to the uncertainty associated with such measurements compared to tracer diffusvities, and further, the phase region in which the interdiffusion was presented was predicted to extend farther into the Al composition range than predicted by Cupid et al. However, the results from the current optimization are in accordance with hypotheses about Ti vacancy concentration governing the diffusivities of Al and Ti as the Ti vacancy concentration is higher than the Al vacancy concentration[17]. Further, as the Ti concentration increases, the Ti vacancy concentration would increase as well, thereby increasing both the Ti and Al diffusivities. Mishin and Herzig[9] further concluded that the vacancy concentration has larger composition dependence at lower temperature, and that there are especially more Ti vacancies than Al vacancies in high Al compositions. This would explain the difference in slope seen between the different temperatures in Figure 4. While these trends are seen in literature and the current optimization, diffusion mechanism variation as function of temperaturerequires further clarification and are left for future studies.

*Nb*

Figure 5 shows the temperature dependence of Nb tracer diffusivity in TiAl(Nb) for different compositions. Like the experimental data suggests, the Nb diffusivity increases with increasing Nb content in the simulations. Divinski et al.[21, 30] concluded that the Nb diffusion is slower than Ti in both TiAl and TiAlNb alloys, but that the diffusivity of both Ti and Nb is higher in the ternary TiAlNb alloy than in the binary TiAl alloy above 1000 K. The diffusivity of Nb in the current optimization is lower than Ti in any alloy, and its compositional dependence is in accordance with that reported by Divinski. However, the Nb concentration dependence of Ti diffusion has the opposite trend.

In the optimized data, the activation energy for Nb diffusion on the Ti sublattice is lower than on the Al sublattice, however the mobility is faster on the Al sublattice. Divinski et al.[21] suggested that the Nb diffusivity in the ternary alloy is 2-3 times slower than the Ti diffusivity, which is thereby slightly different than what was determined in the current optimization. A potential explanation for the difference is site occupancy. While in the current optimization the Nb is allowed to substitute for both Al and Ti, if the Nb were to occupy only Ti sites, as has been suggested by others to occur[27], the current optimization suggest the diffusivity would reduce, since the diffusion activation energy on these sites are higher. The determination of site preference and location of Nb is left for future studies.

The diffusion in several phases of the Ti-Al system has been assessed by Mishin and Herzig[9], including a thorough literature review of experimental data and theoretical calculations. Further, they discuss mechanisms by which diffusion may occur, and determine theoretical activation energies for each. For the γ-phase, their conclusions based on experimental data are that Ti and Al both follow Arrhenius temperature dependence and that Al diffuses slower than Ti and

has higher activation energy. This was accurately captured in the current work. Further, the optimized Nb shows similar temperature dependence but with lower overall diffusivities, which is in complete agreement with that reported by Divinski[21].

**Diffusion couple validation**

The experimental results from the diffusion couple in terms of concentration profiles across the boundary, along with the simulated concentration profiles of the same are shown in Figure 6. Overall the simulated profiles agree with the experimental data, confirming the optimized variables accurately captures physical phenomena. One difference between the experimental profiles and simulated data is that there is a steeper concentration transition of Ti and Nb at the interface for the experimental data.. A potential explanation for the anomaly is texturing effects, skewing the experimental results higher or lower. It is also possible that the vacancy concentration is not uniformly distributed[24], and potentially higher at the boundary/interface, thus locally increasing the diffusivity. The experimental profiles could also include artifacts from the EPMA technique used, in which the electron beam size is approximately 1 um in diameter, thus an average concentration in the area is measured.

**Conclusion**

In this work, a diffusion mobility database for kinetic simulations in the γ-TiAlNb phase was created by a critical assessment of experimental data found in literature, followed by optimization of kinetic parameters. The optimization was further validated experimentally. The optimized parameters are readily available for use with appropriate thermodynamic descriptions, which can thus be used to simulate various diffusion-controlled processes or calculation of multicomponent diffusivities. For practical purposes, descriptions of other phases would be useful to include. Nonetheless, the work presented herein is a database readily usable and also a step towards a complete kinetic description of the TiAlNb system, enabling accelerated alloy and process development.

**Acknowledgements**

The authors would like to acknowledge Professor Hans Seifert and Dr. Damian Cupid at Karlsruhe Institute of Technology for providing the thermodynamic database used in this study, as well as Dr. Henrik Larsson at Thermo-Calc Software for helpful suggestions. Dr. Glenn Bean, Philipp Alieninov and Joshua Wagner at University of Florida are greatly appreciated for assisting with diffusion couple preparation. The work was funded by the US National Science Foundation (NSF), under grant number DMR-0856622 and DMR-1210883.

**References**

[1] C. Leyens, M. Peters, Titanium and titanium alloys, WILEY-VCH GmbH & Co. KGaA, Weinheim, Germany, 2003.
[2] E.A. Loria, Gamma titanium aluminides as prospective structural materials, Intermetallics, 8 (2000) 1339-1345.
[3] D.M. Dimiduk, Gamma titanium aluminide alloys - an assessment within the competition of aerospace structural materials, Materials Science and Engineering a-Structural Materials Properties Microstructure and Processing, 263 (1999) 281-288.
[4] S. Bystrzanowski, A. Bartels, H. Clemens, R. Gerling, F.P. Schimansky, G. Dehm, H. Kestler, Creep behaviour and related high temperature microstructural stability of Ti–46Al–9Nb sheet material, Intermetallics, 13 (2005) 515-524.

[5] R.W. Hayes, B. London, On the creep deformation of a cast near gamma TiAl alloy Ti48Al1Nb, Acta Metallurgica et Materialia, 40 (1992) 2167-2175.
[6] X.J. Xu, L.H. Xu, J.P. Lin, Y.L. Wang, Z. Lin, G.L. Chen, Pilot processing and microstructure control of high Nb containing TiAl alloy, Intermetallics, 13 (2005) 337-341.
[7] O. Rios, S. Goyel, M. Kesler, D. Cupid, H. Seifert, F. Ebrahimi, An evaluation of high-temperature phase stability in the Ti–Al–Nb system, Scr. Mater., 60 (2009) 156-159.
[8] G.E. Bean, F. Ebrahimi, M.V. Manuel, High temperature deformation of Ti-Al-Nb-Cr-Mo alloy with ultrafine microstructure, Intermetallics, 49 (2014) 132-137.
[9] Y. Mishin, C. Herzig, Diffusion in the Ti–Al system, Acta. Mater., 48 (2000) 589-623.
[10] Thermo-Calc, TCS Ti-alloys mobility database v1, 1997.
[11] Thermo-Calc, TCS Al-alloys mobility database v1, 1997.
[12] J.-O. Andersson, J. Agren, Models for numerical treatment of multicomponent diffusion in simple phases, Journal of Applied Physics, 72 (1992) 1350-1355.
[13] O. Redlich, A.T. Kister, Algebraic Representation of Thermodynamic Properties and the Classification of Solutions, Ind. Eng. Chem., 40 (1948) 345-348.
[14] D.M. Cupid, O. Fabrichnaya, O. Rios, F. Ebrahimi, H.J. Seifert, Thermodynamic re-assessment of the Ti-Al-Nb system, International Journal of Materials Research, 100 (2009) 218-233.
[15] J.O. Andersson, T. Helander, L.H. Höglund, P.F. Shi, B. Sundman, Thermo-Calc & DICTRA, Computational Tools for Materials Science, Calphad, 26 (2002) 273-312.
[16] A. Borgenstam, L. Höglund, J. Ågren, A. Engström, DICTRA, a tool for simulation of diffusional transformations in alloys Journal of Phase Equilibria and Diffusion, 21 (2000) 269-280.
[17] C. Herzig, M. Friesel, D. Derdau, S. Divinski, Tracer diffusion behaviour of Ga as an Al-substituting element in Ti3Al and TiAl intermetallic compounds, Intermetallics, 7 (1999).
[18] Y. Song, R. Yang, D. Li, Z.Q. Hu, Z.X. Guo, A first principles study of the influence of alloying elements on TiAl: site preference, Intermetallics, 8 (2000) 563-568.
[19] R.W. Guard, J.H. Westbrook, Aloying behavior of Ni3Al (gamma-phase), Transactions of the American Institute of Mining and Metallurgical Engineers, 215 (1959) 807-814.
[20] Y. Nosé, N. Terashita, T. Ikeda, H. Nakajima, Impurity diffusion in γ-TiAl single crystals, Acta. Mater., 54 (2006) 2511-2519.
[21] S.V. Divinski, C. Klinkenberg, C. Herzig, Tracer Diffusion of Niobium and Titanium in Binary and Ternary Titanium Aluminides, Journal of Phase Equilibria & Diffusion, 26 (2005) 452-457.
[22] R. Kainuma, J. Sato, I. Ohnuma, K. Ishida, Phase stability and interdiffusivity of the L10-based ordered phases in Al-rich portion of the Ti–Al binary system, Intermetallics, 13 (2005) 784-791.
[23] S. Kroll, H. Mehrer, N. Stolwijk, C. Herzig, R. Rosenkranz, G. Frommeyer, Titanium Self-Diffusion in the Intermetallic Compound γ-TiAl, Zeitschrift für metalkunde, 83 (1992).
[24] C. Herzig, T. Przeorski, Y. Mishin, Self-diffusion in γ-TiAl: an experimental study and atomistic calculations, Intermetallics, 7 (1999).
[25] T. Ikeda, H. Kadowaki, H. Nakajima, H. Inui, M. Yamaguchi, M. Koiwa, Tracer-diffusion of 44Ti in TiAl single crystal, Mater. Sci. Eng. A, 312 (2001) 155-159.
[26] S.V. Divinski, S. Frank, U. Södervall, C. Herzig, Solute diffusion of Al-substituting elements in Ni3Al and the diffusion mechanism of the minority component, Acta. Mater., 46 (1998).
[27] Y.L. Hao, D.S. Xu, Y.Y. Cui, R. Yang, D. Li, The site occupancies of alloying elements in TiAl and Ti3Al alloys, Acta. Mater., 47 (1999) 1129-1139.
[28] W. Sprengel, N. Oikawa, H. Nakajima, Single-phase interdiffusion in TiAl, Intermetallics, 4 (1996) 185-189.

[29] C. Herzig, T. Przeorski, M. Friesel, F. Hisker, S.V. Divinski, Tracer solute diffusion of Nb, Zr, Cr, Fe and Ni in γ-TiAl: effect of preferential site occupation, Intermetallics, 9 (2001) 461-472.
[30] S. Divinski, F. Hisker, C. Klinkenberg, C. Herzig, Niobium and titanium diffusion in the high niobium-containing Ti–54Al–10Nb alloy, Intermetallics, 14 (2006) 792-799.

**Table 1**. Summary of datasets used in this paper.

| Experiment | Alloy | Method | D [$m^2/s$] | Q [J/mol] | T [K] | Reference |
|---|---|---|---|---|---|---|
| | | | *Diffusion of Ti* | | | |
| $D^*_{Ti}$ | $Ti_{47}Al_{53}$ | Radiotracer and serial sectioning | $5.2*10^{-6}exp(26.3*10^4/RT)$ | | <1470 | Herzig et al.[24] |
| | $Ti_{46}Al_{54}$ | | $1.5*10^{-5}exp(27.8*10^4/RT)$ | | | |
| | $Ti_{44}Al_{56}$ | | $3.2*10^{-6}exp(26.1*10^4/RT)$ | | | |
| $D^*_{Ti}$ | $Ti_{44}Al_{56}$ | Radiotracer and serial sectioning | $7.1*10^{-6}exp(27*10^4/RT)$ | 273000 | <1470 | Divinski et al.[30] Divinski et al.[21] |
| $D^*_{Ti}$ | $Ti_{44}Al_{56}$ $Ti_{47}Al_{53}$ | Radiotracer and serial sectioning | $7.1*10^{-6}exp(27*10^4/RT)$ | | <1467 | Herzig et al.[24] |
| $D^*_{Ti}$ | $Ti_{36}Al_{54}$ $Nb_{10}$ | Radiotracer | $3.99*10^{-4}exp(-3.0*10^5/RT)$ | 304000 | 1609, 991-1571 | Divinski et al.[30] |
| $D^*_{Ti}$ | $Ti_{46}Al_{54}$ | Radiotracer and serial sectioning | | | 1154-1673 | Kroll et al.[23] |
| $D^*_{Ti}$ | $Ti_{46}Al_{54}$ | Radiotracer Ion beam sputtering | $7.66\times10^{-4}exp(-3.11\pm35*10^5)/RT)$ (⊥) $2.38\times10^{-2}$ $exp(-3.70\pm22*10^5)/RT)$ (//) | | 1133-1307 | Ikeda et al.[25] |
| | | | *Diffusion of Nb* | | | |
| $D^*_{Nb}$ | $Ti_{44}Al_{56}$ | Radiotracer ($^{95}Nb$) and SIMS (ion beam sputtering for $^{93}Nb$) | $1.5*10^{-4}exp(-324000/RT)$ | 324000 | 1059-1643 | Divinski et al.[21] and Herzig et al.[29] |
| $D^*_{Nb}$ | $Ti_{46}Al_{54}$ | Radiotracer | $9.01*10^{-19}$ $2.41*10^{-19}$ $4.85*10^{-20}$ | | 1628 1535 1454 | Herzig et al.[29] |
| $D^*_{Nb}$ | $Ti_{36}Al_{54}$ $Nb_{10}$ | Radiotracer | $1.92*10^{-5}exp(-2.8*10^5/RT)$ | 280000 | 1235-1609 | Divinski et al.[21, 30] |
| | | | *Diffusion of Al* | | | |
| $\widetilde{D}_{TiAl}$ | $Ti_{46}Al_{54}$ | Interdiffusio | | | 1154- | Kroll et al.[23] |

| | | | | | | |
|---|---|---|---|---|---|---|
| | | n / Darken-Manning | | | 1673 | |
| $D_{In}^{*}$ | $Ti_{46.8}Al_{53.2}$ | Radiotracer by In as substitute | | | 1211-1371 | Nose et al.[20] |
| $D_{Ga}^{*}$ | $Ti_{46}Al_{54}$ | Radiotracer by Ga as substitute | | | | Herzig et al.[17] |
| $\widetilde{D}_{TiAl}$ | Interdiffusion $Ti_{50}Al_{50}$ - $Ti_{46}Al_{54}$ | Diffusion couple method | | 295000 | 1116-1583 | Sprengel et al.[28] |
| | | | $1.59*10^{-3}\exp(-3.04*10^{5}/RT)$ (Ti-56Al) | | | |
| $\widetilde{D}_{TiAl}$ | Interdiffusion $Ti_{45}Al_{55}$ - $Ti_{25}Al_{75}$ | Diffusion couple method Boltzmann-Matano | $3.82*10^{-4}\exp(-2.81*10^{5}/RT)$(Ti-60Al) | | 1373-1623 | Kainuma et al.[22] |
| | | | $6.03*10^{-5}\exp(-2.64*10^{5}/RT)$ (Ti-64Al) | | | |

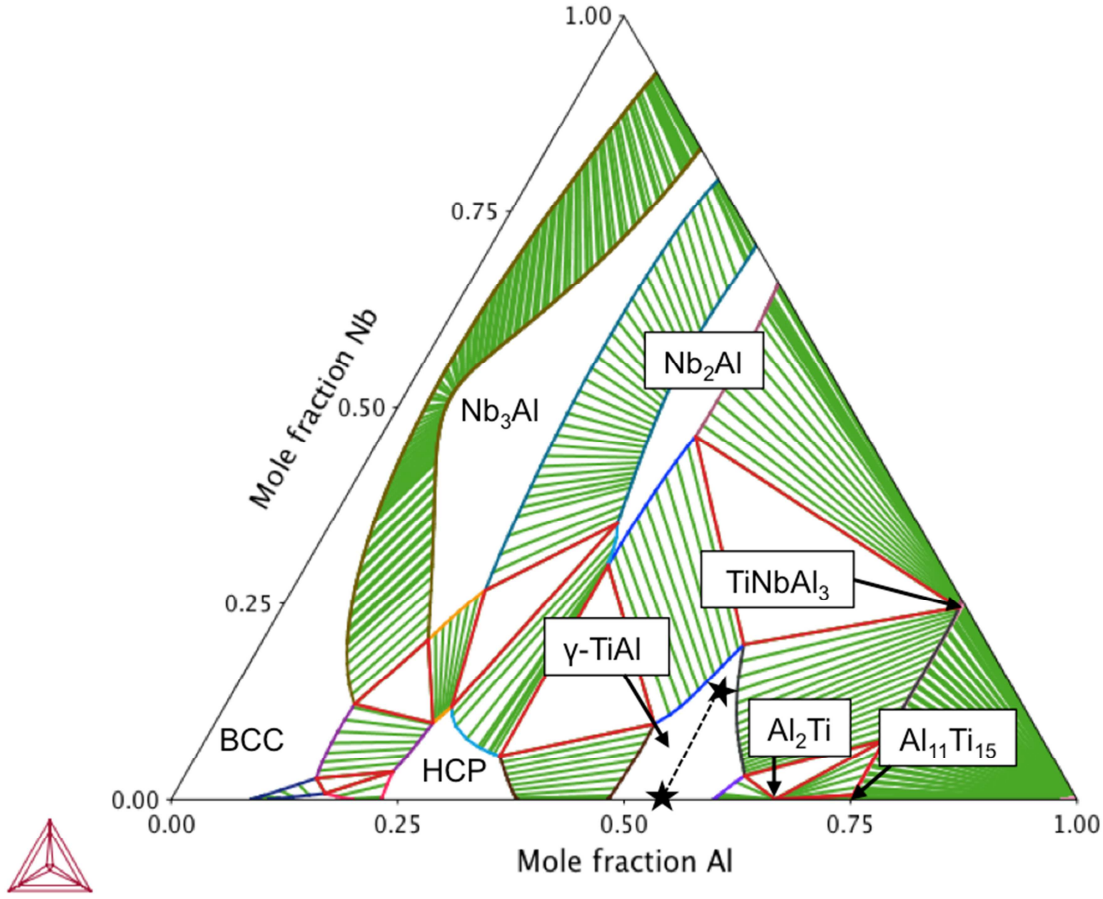


**Figure 1.** Calculated isothermal section of the Ti-Al-Nb system at 1000°C, with alloy compositions used in the validation experiment indicated (star) in the y-TiAl phase region[14][15].

**Table 2**. Optimized mobility parameters in the kinetic database. Note that the Ti-parameter indicated (*) was not optimized, but assigned the same value as the optimized Ti-parameter.

| DICTRA Notation | Mobility Parameter | Value (J/mole) |
|---|---|---|
| | *Ti Diffusivity* | |
| MQ(L10_ALTI&Ti,Al:*) | $\Psi_{Ti}^{Al(Al)}, \Psi_{Ti}^{Al(Nb)}, \Psi_{Ti}^{Al(Ti)}$ | -298256+R*T*LN(8.326E-04) |
| *MQ(L10_ALTI&Ti,Ti:*) | $Q_{Ti}^{Ti(Al)}, Q_{Ti}^{Ti(Nb)}, Q_{Ti}^{Ti(Al)}$ | -298256+R*T*LN(8.326E-04) |
| | *Al Diffusivity* | |
| MQ(L10_ALTI&Al,Al:*) | $\Psi_{Al}^{Al(Al)}, \Psi_{Al}^{Al(Nb)}, \Psi_{Al}^{Al(Ti)}$ | -331142+R*T*LN(9.873E-4) |
| MQ(L10_ALTI&Al,Ti:*) | $\Psi_{Al}^{Al(Al)} \Psi_{Al}^{Ti(Nb)} \Psi_{Al}^{Ti(Ti)}$ | -914053+R*T*LN(8.814E-3) |
| MQ(L10_ALTI&Al,Al,Ti:*) | $A_{Al}^{Al,Ti}$ | -322058+193.8*T |
| | *Nb Diffusivity* | |
| MQ(L10_ALTI&Nb,Ti:*) | $\Psi_{Nb}^{Ti(Al)}, \Psi_{Nb}^{Ti(Nb)}, \Psi_{Nb}^{Ti(Ti)}$ | -684097+R*T*LN(4.214E-03) |
| MQ(L10_ALTI&Nb,Al:*) | $\Psi_{Nb}^{Al(Al))}, \Psi_{Nb}^{Al(Nb)}, \Psi_{Nb}^{Al(Ti)}$ | -284956+R*T*LN(6.104E-4) |

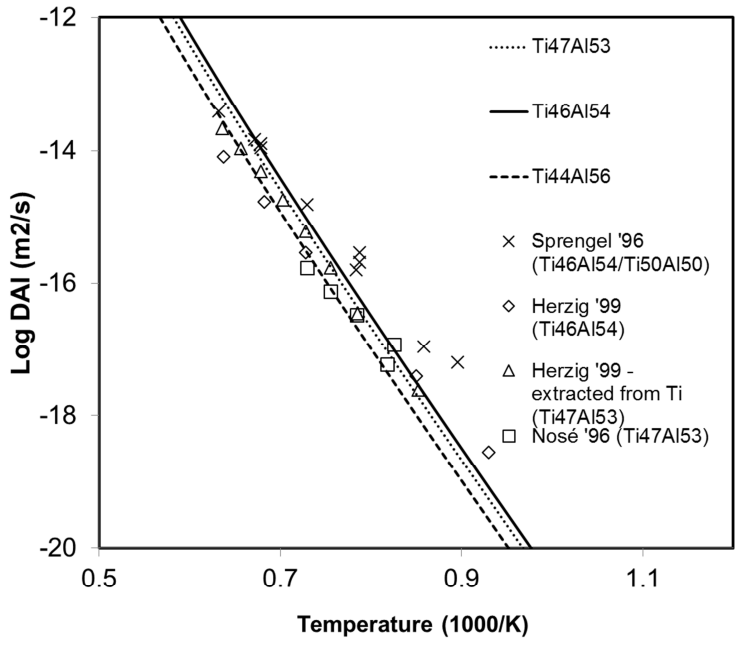


**Figure 2.** Al tracer diffusion as function of temperature, for different stoichiometric compositions. Simulated lines are shown along with experimental data points used in the optimization.

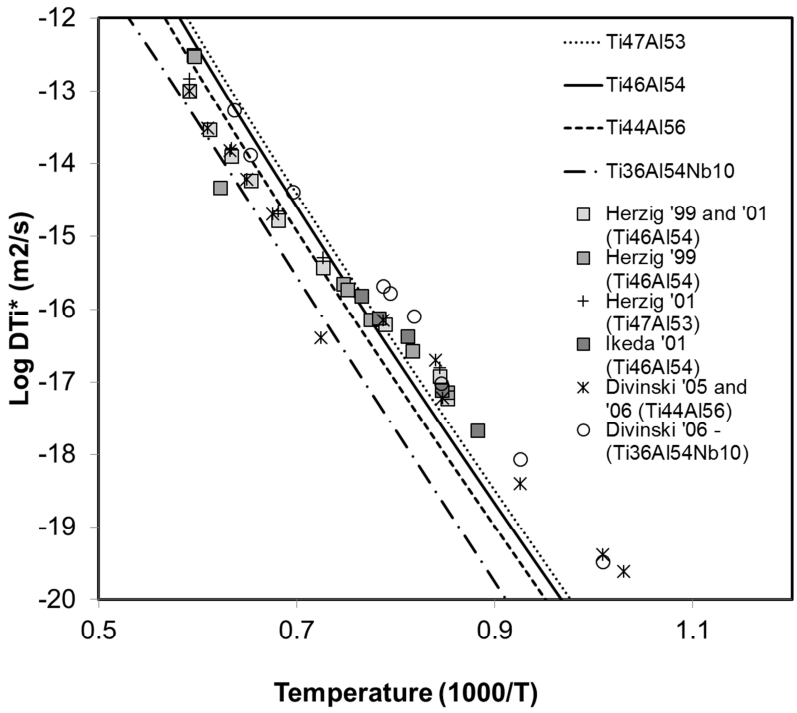


**Figure 3.** Ti tracer diffusion as function of temperature, for different stoichiometric compositions. Simulated lines are shown along with experimental data points used in the optimization.

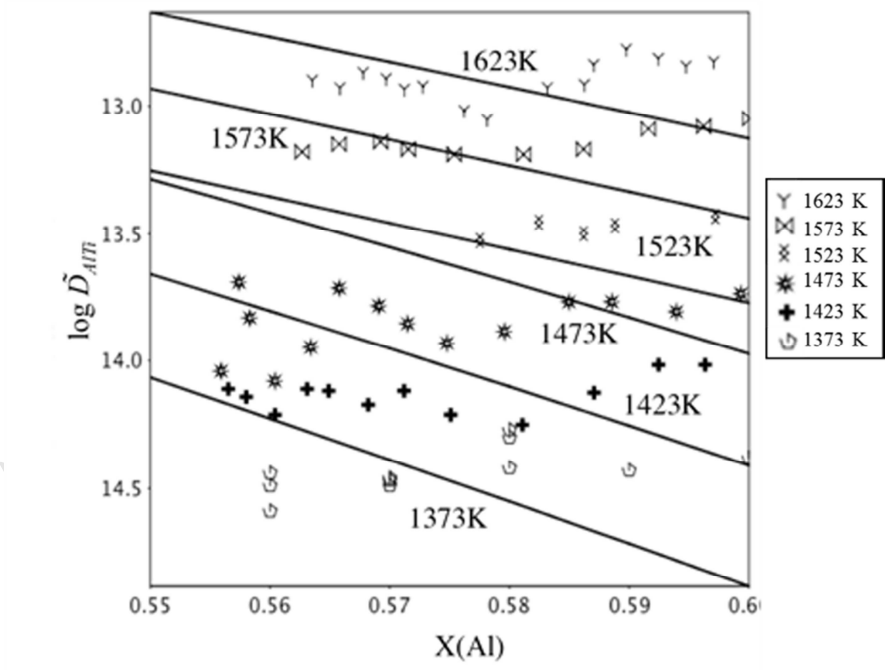

**Figure 4.** TiAl interdiffusion as function of Al content, at different temperatures. Simulated lines are shown along with experimental data points from Kainuma et al.[22] used in the optimization.

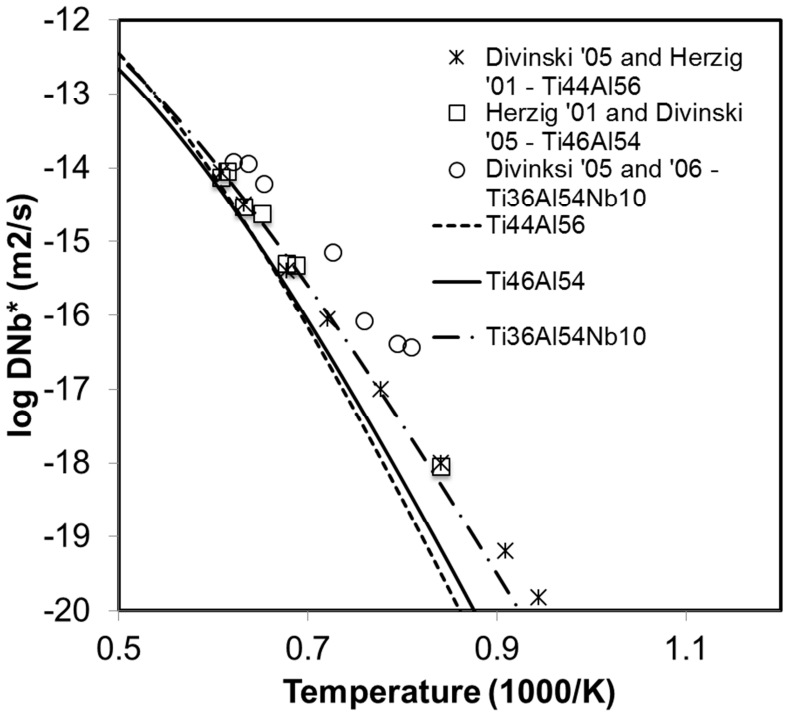


**Figure 5.** Nb tracer diffusivity as function of temperature. Simulated lines are shown along with experimental data points used in the optimization.

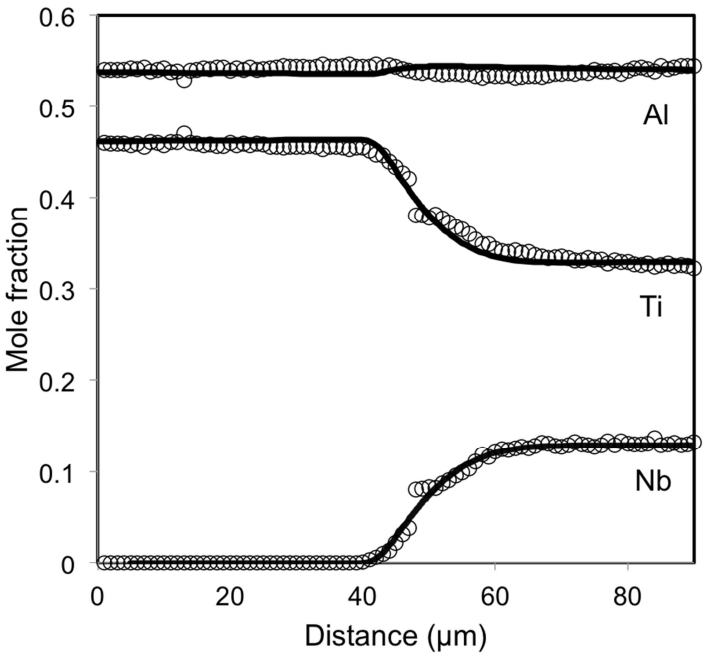

**Figure 6.** Experimental elemental profiles (dotted) obtained from the diffusion couple experiment and EPMA, along with the simulated profiles (lines) obtained using the currently optimized mobility database.

- This is a diffusion mobility database for simulations in the γ-TiAlNb phase.
- Kinetic parameters were optimized and experimentally validated.
- This database can be used to simulate various diffusion-controlled processes.
- This database can be used to calculate multicomponent diffusivities.